

Dynamical scaling behavior in two-dimensional ballistic deposition with shadowing

Jianguo Yu and Jacques G. Amar*

Department of Physics and Astronomy, University of Toledo, Toledo, Ohio 43606

(Received 29 May 2001; revised manuscript received 17 January 2002; published 23 August 2002)

The dynamical scaling behavior in two-dimensional ballistic deposition with shadowing is studied as a function of the angular distribution of incoming particles and of the underlying lattice structure. Using a dynamical scaling form for the surface box number, results for the scaling of the surface fractal dimension are also presented. Our results indicate that, in addition to the usual self-affine universality class corresponding to vertical deposition, there exist at least two additional universality classes characterized by distinct values of the coarsening and roughening exponents p and β describing the evolution of the lateral feature size and surface roughness with film thickness, as well as the surface fractal dimension D_f . For the case of a uniform angular distribution corresponding to an anisotropic flux, we find $p = \beta = 1$ and $D_f \approx 1.7$. However, for ballistic deposition with an isotropic flux (corresponding to a “cosine” angular distribution), we find $p \approx 2/3$ and $D_f \approx 1.5$ while the effective roughening exponent $\beta \approx 0.52\text{--}0.64$ was found to be slightly lattice dependent. In both cases, anomalous scaling of the height-height correlation function is also observed. In contrast, vertical deposition leads to a self-affine surface with $p = 2/3$, $\beta = 1/3$, and $D_f = 1$. The asymptotic scaling behavior appears to depend on the behavior of the angular distribution at large angles but does not depend on other details. An analysis that clarifies the relationship between the launch angle distribution used in the simulations and the flux distribution is also presented.

DOI: 10.1103/PhysRevE.66.021603

PACS number(s): 81.15.Aa, 68.55.-a, 05.10.Ln, 81.15.Cd

I. INTRODUCTION

The evolution of the surface morphology during the growth and deposition of thin films has been a subject of intense interest for the last few years [1,2]. As a result, a variety of simple models have been studied. One example is the ballistic deposition model [2,3] that corresponds to the irreversible “sticking” of particles to the growing film. Ballistic deposition with vertical deposition has been extensively studied [2], and is known to lead to a self-affine surface morphology whose scaling behavior corresponds to the Kardar-Parisi-Zhang (KPZ) equation [4]. In two dimensions, the corresponding scaling exponents are known exactly to be $\alpha = 1/2$, $\beta = 1/3$, and $p = 2/3$, where α is the roughness exponent corresponding to the dependence of the surface roughness or rms surface width w on lateral length scale L (i.e., $w \sim L^\alpha$), the exponent β describes the growth of the surface roughness w with time (i.e., $w \sim t^\beta$), and p is the coarsening exponent corresponding to the growth of the lateral surface correlation length or feature size ξ (i.e., $\xi \sim t^p$).

While vertical deposition leads to a self-affine surface, deposition with a distribution $P(\theta)$ of deposition angles with respect to the substrate normal leads to an instability known as the shadow instability [5,6]. The shadow instability is due to the fact that parts of the surface that “stick out” may shadow nearby points, thus retarding their growth. In the case of low-temperature sputter deposition of amorphous and polycrystalline thin films, the shadow instability is known to play a significant role in determining the surface morphology [7–10]. As a result, the effects of the shadow instability on the surface morphology have been extensively studied in a variety of continuum and discrete models [5,6,11–23]. In particular, for the case of two-dimensional ballistic deposi-

tion with particles launched (sequentially) from a “fixed” height above the surface with a uniform angular distribution, discrete off-lattice simulations by Tang and Liang [19] yielded an effective value of the roughening exponent $\beta \approx 0.7$, whose value appeared to be approaching 1. However, as shown in the Appendix and discussed in Sec. II (see also Ref. [23]) such a uniform “launch angle” distribution does not correspond to an uniform flux of particles above the surface but rather to a nonuniform flux distribution $J(\theta) \sim 1/\cos(\theta)$, where θ is the angle between the direction of incidence and the substrate normal. Similar results (i.e., $p = \beta = 1$) have also been obtained by Yao *et al.* [17] from numerical integration of the two-dimensional KPZ equation (which includes the effects of surface tension, noise, and sideways growth) in the presence of shadowing with a similar flux distribution [24].

We note, however, that for sputter deposition, the angular distribution of atoms sputtered from the target is not typically uniform but in many cases may be approximated by a “cosine” distribution [22,25]. Assuming a low gas/plasma pressure, so that collisions with the gas can be neglected, such a distribution implies an *isotropic* flux of particles arriving at the surface (see the Appendix). Such an isotropic flux distribution is also expected in the case of low-pressure chemical vapor deposition [23], as well as in the case of sputter deposition at high gas pressure due to the collisions of particles with the gas. However, the scaling behavior of ballistic deposition in the presence of such an isotropic flux has not been studied.

In this paper we present results for the scaling behavior of the surface morphology for the case of two-dimensional ballistic deposition with an isotropic flux distribution, as well as for an anisotropic flux [$J(\theta) \sim 1/\cos(\theta)$] corresponding to a uniform launch angle distribution above the surface. In addition, using a dynamical scaling form, we present results for the dynamical scaling of the surface fractal dimension. Our

*Electronic address: jamar@physics.utoledo.edu

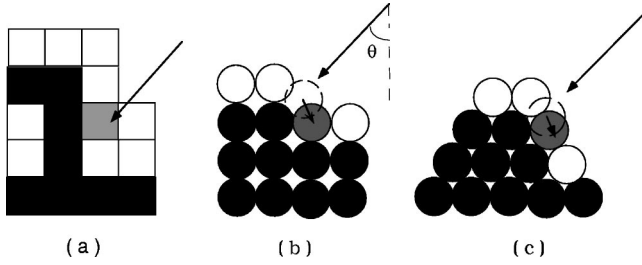


FIG. 1. Schematic showing ballistic deposition models studied: (a) square-lattice box model, (b) square-lattice disk model, and (c) triangular-lattice disk model. Arrows indicate particle trajectory and shaded squares (circles) indicate final sticking sites. Open circles in (b) and (c) indicate potential sticking sites.

results indicate that, in addition to the usual self-affine universality class corresponding to vertical deposition, in the presence of shadowing there exist at least two additional distinct universality classes. The scaling behavior in each universality class is independent of the lattice microstructure or other details but depends on the angular distribution.

II. MODEL

In order to study the dependence of the surface morphology and scaling behavior on the lattice geometry, we have studied ballistic deposition on two different lattices, a square lattice and a triangular lattice. In both cases, the depositing particles were released from a random position along a line of the same length L as the substrate, which was parallel to the substrate but above the highest point of the surface, with the appropriate angular distribution $P(\theta)$ where θ is the angle between the substrate normal and the direction of incidence (see Fig. 1). As shown in the Appendix, the angular dependence of the resulting flux $J(\theta)$ may be simply related to the launch angle distribution $P(\theta)$ using the relation

$$J(\theta) \sim P(\theta)/\cos(\theta). \quad (1)$$

Thus a uniform launch angle distribution $P(\theta) \sim \text{const}$ corresponds to an anisotropic flux distribution $J(\theta) \sim 1/\cos(\theta)$ while a cosine launch angle distribution $P(\theta) \sim \cos(\theta)$ corresponds to an isotropic flux. For the case of a uniform angular distribution, one has $P(\theta) = 1/\pi$ for $-\pi/2 \leq \theta \leq \pi/2$ and $P(\theta) = 0$ otherwise, and the deposition angle was randomly selected with the appropriate weight using the expression $\theta = \pi(r - 1/2)$, where r is a uniform random number between 0 and 1. For the case of an isotropic flux corresponding to a cosine launch angle distribution, one has $P(\theta) = \frac{1}{2}\cos\theta$ for $-\pi/2 \leq \theta \leq \pi/2$ and $P(\theta) = 0$ otherwise, and the deposition angle θ was determined using the expression $\theta = \arcsin(2r - 1)$ where again r is a uniform random number between 0 and 1.

In the case of a square lattice, two different models were studied—a “box” model [see Fig. 1(a)] and a square-lattice “disk” model [see Fig. 1(b)]. In the box model, particles are assumed to travel ballistically (off lattice) until they enter a box that is a nearest neighbor to an occupied site. Once this occurs the corresponding box is occupied [see Fig. 1(a)]. In

the square-lattice disk model, the particles are assumed to be disks of uniform radius and again follow a ballistic off-lattice trajectory until contacting the surface. The depositing particle is then moved to the lattice position nearest to the point of contact. In the triangular lattice simulations a disk model was also used but after reaching the surface the particles were moved to the nearest unoccupied site on a triangular lattice [see Fig. 1(c)] corresponding to a site with one or more occupied nearest neighbors. In this case, two different models, a “one-bond” model and a “two-bond” model were studied. In the one-bond model the depositing particle was moved to the nearest lattice site regardless of the number of bonds, while in the two-bond model the particle was moved to the nearest lattice site with at least two nearest-neighbor bonds. In all cases, the initial condition was a flat substrate.

In order to study the dependence of the surface morphology on the angular distribution a variety of quantities were measured as a function of average film height $\langle h \rangle$. These included the root-mean-square (rms) height fluctuations of the surface or surface width $w = \langle (h - \langle h \rangle)^2 \rangle^{1/2}$ [where $h(x)$ is the maximum height of the surface at position x along the substrate] as well as the height-height correlation function $G(x) = \langle \tilde{h}(0)\tilde{h}(x) \rangle$, where $\tilde{h}(x) = h(x) - \langle h \rangle$ and the height-difference correlation function $G_2(x) \equiv \langle (h(x) - h(0))^2 \rangle$ were calculated. The typical lateral surface correlation length ξ was determined by calculating the value of x corresponding to the first zero crossing of $G(x)$ [26]. From the dependence of the correlation length ξ on film thickness the coarsening exponent p , where $\xi \sim \langle h \rangle^p$, was determined. Similarly the surface width w was used to determine the roughening exponent β where $w \sim \langle h \rangle^\beta$.

In order to characterize the surface morphology the roughness exponent α , where $G(r) \sim r^{2\alpha}$ and the surface fractal dimension D_f were also determined. In addition, the cluster size or “tree” distribution [27] $n(s)$ corresponding to the number of clusters of size s was also measured. As in previous work on related models [27,30], we identify all newly deposited particles that attach to the substrate in the first layer and which have no neighbors in that layer, as corresponding to seed particles for a new cluster. Any particle attaching to a given seed or cluster is assigned to that cluster. In the case in which a newly deposited particle simultaneously attaches to two or more different clusters, then the cluster to which it is assigned is randomly chosen.

In order to minimize finite-size effects, which are particularly strong due to shadowing for the case of a uniform angular distribution, both periodic boundary conditions and very large system sizes were used, while typically 1000 layers were deposited. To allow simulations of such large system sizes and film thicknesses, a “bit” packing technique (in which one 16-bit word represented 16 different lattice sites) was used in order to conserve memory.

III. RESULTS

A. Uniform launch angle distribution

Figure 2 shows our results for the surface coarsening and roughening behavior as a function of film thickness for the

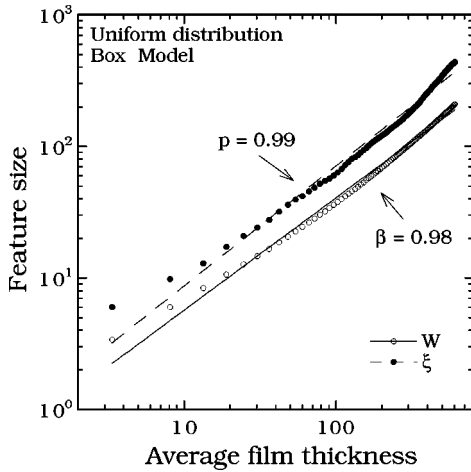


FIG. 2. Surface width w and lateral feature size ξ as functions of average film thickness $\langle h \rangle$ for the square-lattice box model with a uniform angular distribution ($L = 32\,768$).

case of ballistic deposition with a uniform angular distribution $P(\theta)$ using the square-lattice box model. As can be seen, in this case both the roughening exponent β and the coarsening exponent p are approximately equal to 1. These results are consistent with the off-lattice simulation results of Tang and Liang [19] who found $\beta = 0.7$ but which seemed to be increasing with increasing film thickness. Interestingly, the result $p = 1$ also agrees with recent theoretical predictions for the “grass” model [18] corresponding to growth of a random substrate with a uniform angular distribution in the absence of noise, even though there is no sideways growth in this model. As already noted, this result is also in agreement with numerical integration results [17] for the KPZ equation with shadowing and a uniform angular distribution [24]. The large values of β and p obtained in these models are clearly due to the very large flux [$J(\theta) \sim 1/\cos(\theta)$] at large angles of incidence with respect to the substrate normal.

B. Cosine launch angle distribution

We now consider the scaling behavior of the surface morphology for the case of ballistic deposition with a cosine angular distribution which corresponds to an isotropic flux $J(\theta) = \text{const}$ for $-\pi/2 < \theta < \pi/2$ and $J(\theta) = 0$ otherwise. As shown in Fig. 3 for the box model, in this case we find significantly smaller values for the corresponding exponents, i.e., $p \approx \beta \approx 2/3$. As an independent estimate of the coarsening exponent p , we have also measured the dependence of the density ρ of “surface” clusters on the average film height $\langle h \rangle$, where a surface cluster is a nearest-neighbor connected cluster (as defined in Sec. II) which contains at least one particle at the surface of the film. Since $1/\rho$ is the average lateral surface cluster size, we expect that $\rho \sim 1/\xi \sim \langle h \rangle^{-p}$. As can be seen in Fig. 4, the resulting value for the coarsening exponent $p \approx 0.69$ agrees well with that obtained in Fig. 3 using the height-height correlation function. Similar results (i.e. $p \approx \beta \approx 2/3$) have also been obtained (see Fig. 5) for the square-lattice disk model with a cosine angular distribution

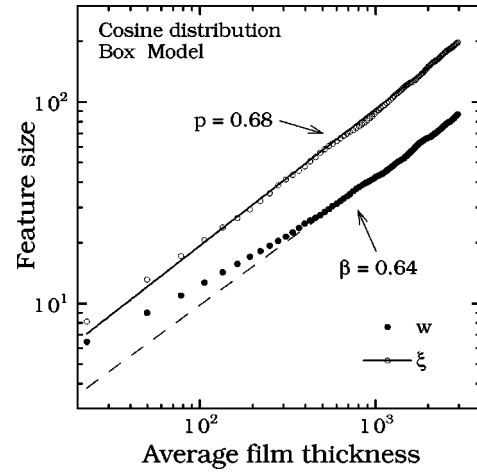


FIG. 3. Same as Fig. 2 but for cosine distribution.

although in this case the effective roughening exponent $\beta \approx 0.64$ appears to be somewhat lower than the coarsening exponent p .

In order to investigate the lattice dependence of the coarsening and roughening behavior in the case of a cosine distribution, we have also carried out simulations using the triangular lattice disk model for both the one-bond and two-bond cases. As can be seen in Fig. 6, in both cases we again find $p \approx 2/3$ that is in good agreement with our results for the square-lattice box and disk models. However, the corresponding values for the roughening exponent $\beta \approx 0.55 \pm 0.03$ are somewhat smaller. While this may indicate that the asymptotic growth exponent β is weakly lattice dependent, it is more likely due to a significantly slower crossover to the asymptotic value for the triangular lattice.

C. Cluster-size distribution exponent τ

In order to determine the cluster-size distribution exponent τ [where $n(s) \sim s^{-\tau}$ is the number of clusters of size s] for the case of an isotropic flux, we have measured the cluster-size distribution for a cosine angular distribution (box model). As can be seen in Fig. 7, the value of τ (i.e., $\tau \approx 7/5$) is the same as for the case of vertical deposition [28] and is consistent with the scaling prediction [28,29], $\tau = 2 - [1/(1+p)]$ with $p = 2/3$. We note that the result $\tau \approx 3/2$ obtained in Ref. [19] for a uniform angular distribution is also consistent with this scaling relation with $p = 1$ as obtained in our simulations.

D. Dynamic scaling of the surface-fractal dimension

Figure 8 shows typical morphologies for small system size ($L = 256$) obtained for the (two-bond) triangular-lattice disk model for the cases of (a) vertical ballistic deposition, (b) deposition with a cosine distribution corresponding to an isotropic flux, and (c) deposition with a uniform angular distribution after 40 ML have been deposited. Similar pictures have also been obtained for the square-lattice disk model and the box model. In all cases the resulting films are “compact,” as indicated by the linear relation between the number of deposited layers and the average film height $\langle h \rangle$ [31].

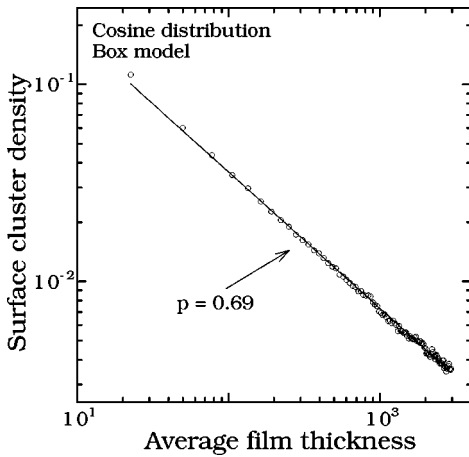


FIG. 4. Surface cluster density ρ as a function of film thickness for the square-lattice “box model” and a cosine distribution.

However, as can be seen in Fig. 8, as the “width” of the angular distribution increases, the resulting films become “rougher” and more “open” in structure. In particular, the many “valleys” and “fjords” of different sizes in the case of an cosine or a uniform distribution suggest that in the presence of shadowing the film surface itself may be fractal.

In order to quantitatively characterize the surface morphology as a function of film thickness, we have calculated the surface fractal dimension D_f for both a uniform angular distribution and a cosine distribution using the box-counting method [1,32] along with the assumption of dynamical scaling [33]. For a surface that is roughening during growth, one expects that the range of length scales over which fractal behavior may be observed should increase with film thickness as the typical lateral feature size, i.e., as $\xi \sim t^p$. If $N(l,t)$ corresponds to the number of boxes of size l and dimension $d+1$ containing a surface particle at time t , then one expects $N(l,t) \sim l^{-D_f}$ for $l \ll \xi(t)$ and $N(l,t) \sim l^{-d}$ (where $d=1$ is the dimension of a flat surface) for $l \gg \xi(t)$. Combining these observations with the assumption of scaling leads to the following dynamical scaling form for the surface box number

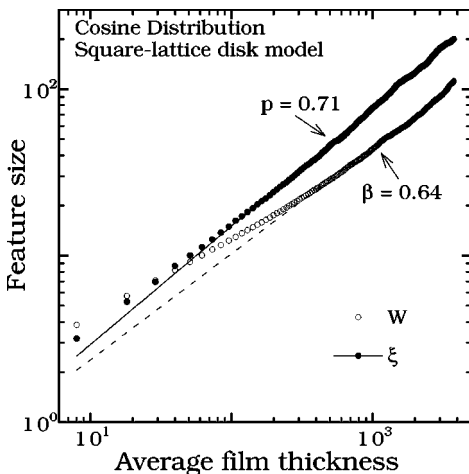


FIG. 5. Surface width w and lateral feature size ξ as functions of film thickness $\langle h \rangle$ for the square-lattice disk model with a cosine angular distribution ($L=131\,072$).

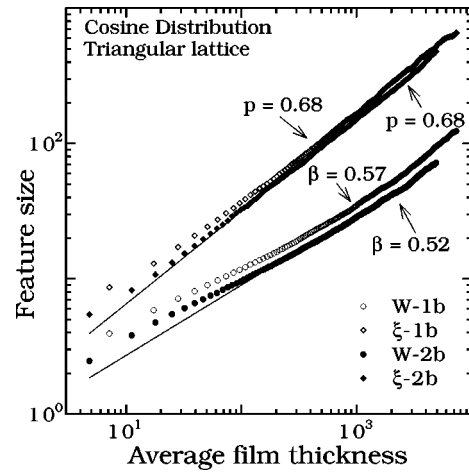


FIG. 6. Surface width and lateral feature size as functions of film thickness for the triangular-lattice model with a cosine angular distribution ($L=262\,144$). Open symbols correspond to the one-bond model (1b) while filled symbols correspond to the two-bond model (2b).

$N(l,t)$ as a function of box size l and film thickness or time t :

$$N(l,t) = t^{-dp} f(l/t^p), \quad (2)$$

where the dynamic scaling function $f(u)$ satisfies $f(u) \sim u^{-d}$ for $u \gg 1$ and $f(u) \sim u^{-D_f}$ for $u \ll 1$.

Figure 9 shows our results for the dynamic scaling function $f(u)$ obtained using the square-lattice box model for both angular distributions. [Note that in Figs. 9 and 10, $N(l)$ is actually the number of boxes of size l divided by the system size L where either $L=655\,36$ or $L=131\,072$.] In both cases there is excellent scaling. For the case of a uniform angular distribution we find $D_f \approx 1.7$, while for the case of a cosine distribution corresponding to a uniform flux above the surface we find $D_f \approx 1.5$.

In contrast, for the case of vertical deposition (not shown) while the surface appears to be fractal over short length scales, the range of box sizes over which fractal scaling may be observed does not increase with film thickness, and so the

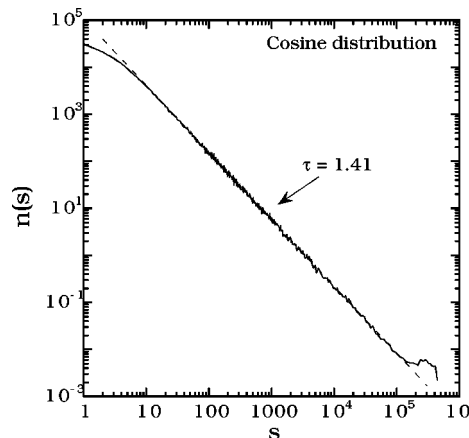


FIG. 7. Cluster-size distribution $n(s)$ for the square-lattice box model with cosine distribution after 1000 layers have been deposited ($L=16\,384$, 40 runs).

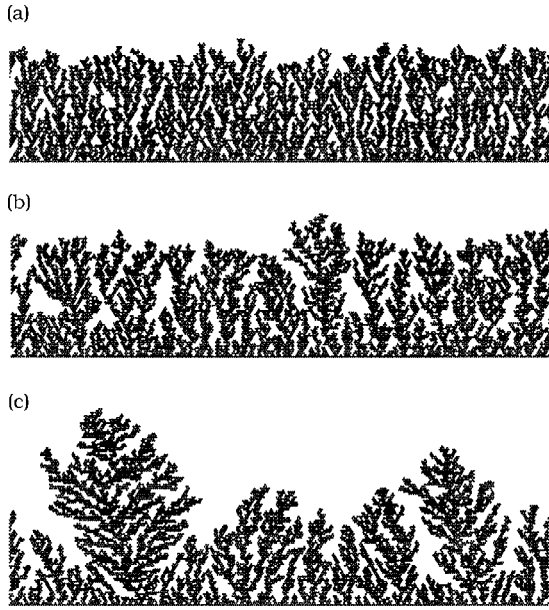


FIG. 8. Typical morphologies obtained in triangular-lattice disk model simulations after 40 ML have been deposited ($L=256$): (a) vertical deposition, (b) cosine distribution, and (c) uniform distribution.

surface is self-affine [2]. Thus, even though the value of the coarsening exponent is essentially the same ($p \approx 2/3$) for both vertical deposition and the cosine distribution, the cosine distribution leads to a fractal surface while vertical deposition does not. Figure 10 shows similar results for the case of a triangular lattice with a cosine distribution for both the one-bond model and the two-bond model. In this case, one again has $D_f \approx 1.5$ for a cosine distribution. This suggests that the surface-fractal dimension D_f is in fact universal, i.e., independent of the lattice geometry for a given angular distribution $P(\theta)$.

E. Anomalous dynamical scaling and multiscaling

In order to further investigate the surface morphology we have also measured the surface roughness exponent α for both a cosine distribution and a uniform distribution. Figure 11 shows the height-difference correlation function $G_2(r)$ at two different coverages for both the square-lattice box model and the triangular-lattice model for both distributions. As can be seen, the effective roughness exponent $\alpha \approx 1/2$ [34] is significantly smaller than the value $\alpha \approx 1$ predicted by the usual Family-Vicsek scaling relation [33] $\alpha = \beta/p$, thus indicating anomalous scaling [35–37]. The existence of anomalous scaling is further confirmed by the dependence of the height-height correlation function $G_2(r)$ on film thickness even for small r and is likely due to the fractal nature of the surface, which leads to overhangs and results in large discontinuities in the maximum surface height as a function of position.

The existence of anomalous scaling also suggests the possibility of multiscaling [38]. In order to investigate this possibility, we have also calculated the generalized roughness exponent α_n where $G_n(r) = \langle [h(r) - h(0)]^n \rangle \sim r^{n\alpha_n}$ for the

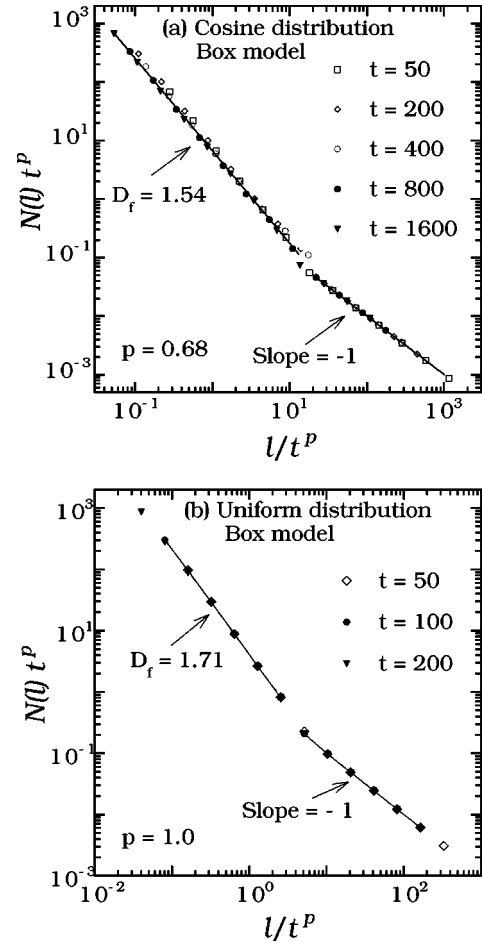


FIG. 9. Surface-fractal-dimension dynamic scaling function $f(l/t^p)$ for the square-lattice box model with (a) cosine angular distribution and (b) uniform angular distribution.

square-lattice box model with a cosine distribution. As can be seen in Fig. 12, the strong dependence of α_n on n indicates strong multiscaling behavior that is again due to the fractal nature of the surface.

IV. DISCUSSION

We have studied the dynamic scaling behavior of the surface in two-dimensional ballistic deposition with shadowing as a function of both the angular distribution $P(\theta)$ and the underlying lattice structure. Our results demonstrate the existence of at least two distinct universality classes in addition to the usual self-affine universality class ($\alpha = 1/2, \beta = 1/3, p = 2/3$) corresponding to vertical deposition. In particular for the case of a uniform angular distribution, we found $p \approx \beta \approx 1$ (square-lattice box model). This result is consistent with earlier off-lattice simulations by Tang and Liang [19]. The result $p = 1$ also agrees with recent theoretical predictions for the “grass” model [18] corresponding to growth with a uniform angular distribution in the absence of noise, even though there is no sideways growth in this model. Thus it appears that for the case of a uniform distribution in two dimensions, the scaling exponents p and β are universal, i.e., independent of the underlying lattice structure. As already

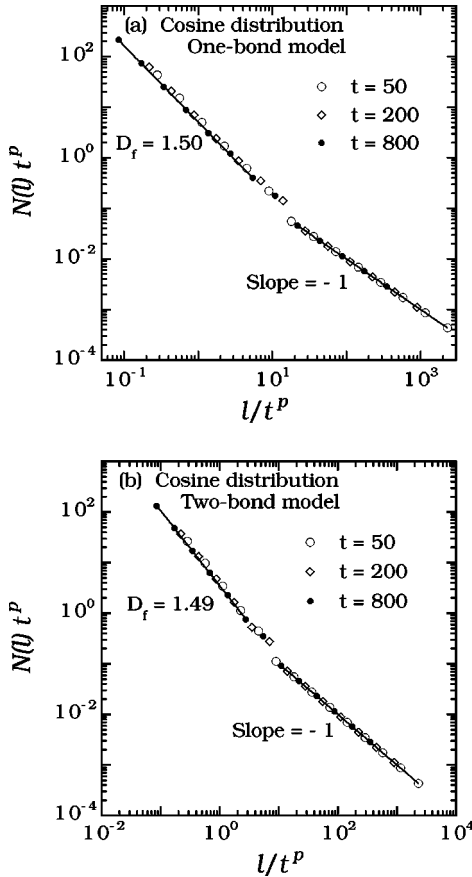


FIG. 10. Surface-fractal-dimension dynamic scaling function $f(l/t^p)$ for the triangular-lattice disk model with a cosine angular distribution for (a) the one-bond model and (b) the two-bond model.

noted, such a distribution corresponds to an anisotropic flux distribution $J(\theta) \sim 1/\cos(\theta)$ and the large values of β and p are due to the large flux at high angles of incidence. We note that these results do not agree with the dimension-independent prediction $p=3/4$ obtained by Tang *et al.* [11] for coarsening in the presence of noise. The discrepancy is most likely due to the neglect of shadowing in these arguments.

In contrast, for a cosine angular distribution, corresponding to a uniform flux above the surface, we found $p \approx 2/3$ independent of the lattice studied. These results indicate that for a given angular distribution $P(\theta)$, the coarsening exponent is universal and does not depend on the details of the system. Similarly, the measured values for the effective surface roughening exponent β were found to be significantly different than for a uniform distribution. For the square-lattice box model and disk models, we found $\beta \approx p \approx 2/3$. However, for the triangular-lattice models the effective roughening exponent β was found to be slightly lower, i.e., $\beta \approx 0.52-0.57$. While this may indicate that the asymptotic growth exponent is weakly lattice dependent, it is more likely due to a significantly slower crossover to the asymptotic value for the triangular lattice.

We note that the existence of distinct universality classes for coarsening is consistent with the ‘‘Huygen’s principle’’ picture of Tang *et al.* [11], which indicates that microscopic

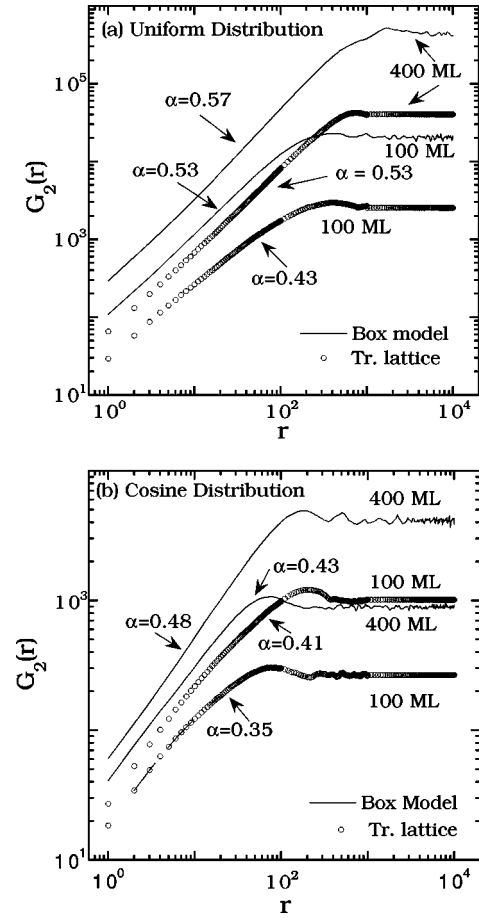


FIG. 11. Height-difference correlation function $G_2(r)$ for the square-lattice box model (filled symbols) and two-bond triangular-lattice model (solid lines) at 100 ML and 400 ML coverage ($L = 131\,072$) for (a) uniform distribution and (b) cosine distribution.

details do not affect the lateral coarsening behavior. However, this leaves open the question of how the coarsening exponent depends on the angular distribution. We note that Krug and Meakin [18] have shown that for the deterministic ‘‘grass’’ model with random initial conditions, one has $p = 1$ for $V(\pi - \theta) \sim (\pi - \theta)^x$ if $x \leq 1$ where $V(\theta)$ is the local growth rate as a function of exposure angle θ . In analogy to this work, we conjecture that depending on the behavior of $P(\theta)$ for large θ , either the KPZ universality class ($p = 2/3, D_f = 1$) or the cosine universality class ($p = 2/3, D_f = 3/2$) or the uniform universality class ($p = \beta = 1, D_f \approx 1.7$) will be selected. As a test of this conjecture, we have also carried out simulations for the triangular-lattice (one-bond) disk model with an angular distribution $P(\theta)$ that decays linearly to zero at $\theta = \pm \pi/2$ [i.e., $P(\theta) = (2/\pi)(1 - 2|\theta/\pi|)$] and obtained scaling exponents ($p \approx 2/3, D_f \approx 3/2$) in good agreement with our results for a cosine distribution. The simulations of Tang and Liang [19] using a uniform distribution up to some maximum angle θ_m , which indicated a transition from KPZ behavior to the uniform distribution universality class at a critical value of $\theta_m \approx 80^\circ$, are also consistent with this conjecture. However, further work will be needed to study more carefully the dependence of the universality class on the distribution.

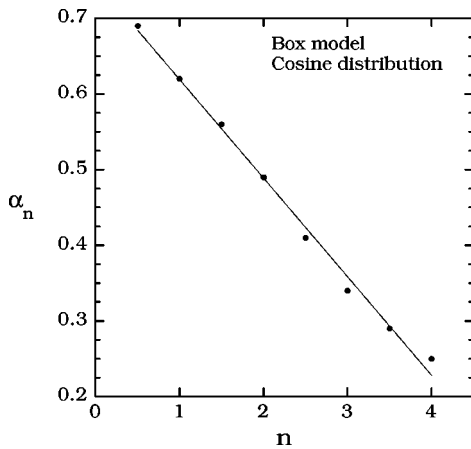


FIG. 12. Generalized roughness exponent α_n as a function of n for the square-lattice box model with a cosine distribution.

We have also used a dynamical scaling form for the surface box number $N(l, t)$ to study the fractal-surface morphology in the presence of shadowing. Using this dynamical scaling form, we have shown that even though the resulting film is compact, for both a cosine and a uniform angular distribution, the surface itself is fractal. In addition, the surface fractal dimension D_f appears to be independent of the lattice geometry for a given angular distribution $P(\theta)$. In particular, we found $D_f \approx 1.7$ for the case of a uniform distribution and $D_f \approx 1.5$ for the case of a cosine distribution. These results are in contrast to the case of vertical deposition for which $D_f = 1$. As a consequence of the fractal morphology of the surface, anomalous scaling for the height-difference correlation function $G_2(r)$ as well as multiscaling of the generalized local roughness exponent α_n were observed.

It is interesting to note that the surface fractal dimension $D_f \approx 1.7$ obtained for a uniform angular distribution is very close to that obtained for diffusion-limited aggregation [39] in two dimensions. That this is the case may not be surprising since ballistic deposition with a uniform angular distribution is essentially equivalent to a diffusion-limited aggregation process for which the diffusion length is significantly larger than the feature size. Due to this difference, diffusion-limited aggregation leads to clusters that are mass fractals as well as surface fractals. Similarly, we note that the value $D_f \approx 1.5$ obtained for a cosine distribution is identical to the “local” fractal dimension $D_{loc} = 2 - \alpha = 3/2$ for the case of ordinary (vertical) ballistic deposition. Thus, one may think of the effect of shadowing in this case as converting a local surface-fractal dimension into a global surface-fractal dimension. Such a connection is consistent with the fact that the “coarsening” exponent $p \approx 2/3$ is the same in both cases.

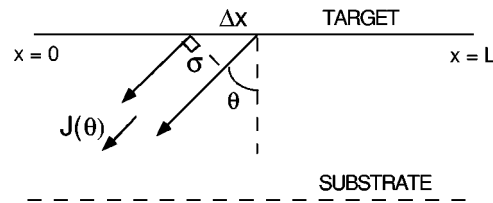


FIG. 13. Schematic showing deposition geometry corresponding to particles “launched” from a random position x along the target line above the substrate with angular distribution $P(\theta)$. Arrows correspond to a flux tube of cross section σ at an angle θ with respect to the substrate normal.

In conclusion, our results show that while shadowing plays a significant role in determining the surface morphology in two-dimensional ballistic deposition, there appear to be only a finite number of distinct universality classes. For the case of a uniform angular distribution corresponding to an anisotropic flux, our results confirm that $p = \beta = 1$ [17,19], while the surface-fractal dimension $D_f \approx 1.7$ is the same as for diffusion-limited aggregation. In contrast, for the case of a uniform flux above the surface, our results indicate the existence of a new universality class with $p \approx \beta \approx 2/3$ and $D_f \approx 3/2$, although a slight dependence of the effective growth exponent β on the lattice was observed. We have also presented an analysis that clarifies the connection between the launch angle distribution $P(\theta)$ and the flux distribution $J(\theta)$. In the future we plan to investigate the dependence of the surface morphology on the angular distribution in three-dimensional models of ballistic deposition in order to obtain a better understanding of the role of shadowing in low-temperature sputter deposition.

ACKNOWLEDGMENTS

This research was supported by the Petroleum Research Fund of the American Chemical Society. Part of this work was carried out using the computational facilities of the Ohio Supercomputer Center.

APPENDIX: CONNECTION BETWEEN LAUNCH ANGLE DISTRIBUTION $P(\theta)$ AND FLUX DISTRIBUTION $J(\theta)$

As shown in Fig. 13, particles are sequentially launched from a random position $0 \leq x \leq L$ along the “target” line of length L above the substrate with an angular distribution $P(\theta)$. Consider a flux “tube” of cross-sectional “area” σ which makes an angle θ with respect to the substrate normal as shown in Fig. 13. The total flux $J(\theta)$ of particles passing through such a tube is proportional to the target or launch area $\Delta x = \sigma / \cos(\theta)$, divided by the flux-tube cross-sectional area σ , times the probability $P(\theta)$ that particles are launched at angle θ . Thus, one has $J(\theta) \sim P(\theta) / \cos(\theta)$.

- [1] A.-L. Barabasi and H.E. Stanley, *Fractal Concepts in Surface Growth* (Cambridge University Press, New York, 1995).
 [2] P. Meakin, *Fractals, Scaling and Growth far from Equilibrium* (Cambridge University Press, New York, 1998).

- [3] M.J. Vold, *J. Colloid Sci.* **14**, 168 (1959).
 [4] M. Kardar, G. Parisi, and Y.C. Zhang, *Phys. Rev. Lett.* **56**, 889 (1986).
 [5] R.P.U. Karunasiri, R. Bruinsma, and J. Rudnick, *Phys. Rev.*

- Lett. **62**, 788 (1989).
- [6] G.S. Bales and A. Zangwill, Phys. Rev. Lett. **63**, 692 (1989).
- [7] R.A. Roy and R. Messier, Mater. Res. Soc. Symp. Proc. **38**, 363 (1985).
- [8] R. Messier and J.E. Yehoda, J. Appl. Phys. **58**, 3739 (1985).
- [9] R. Messier, J. Vac. Sci. Technol. A **4**, 490 (1986).
- [10] T. Salditt *et al.*, Europhys. Lett. **36**, 565 (1996).
- [11] C. Tang, S. Alexander, and R. Bruinsma, Phys. Rev. Lett. **64**, 772 (1990).
- [12] G.S. Bales, R. Bruinsma, E.A. Eklund, R.P.U. Karunasiri, and A. Zangwill, Science **249**, 265 (1990).
- [13] G.S. Bales, and A. Zangwill, J. Vac. Sci. Technol. A **9**, 145 (1991).
- [14] C. Roland and H. Guo, Phys. Rev. Lett. **66**, 2104 (1991).
- [15] L. Golubovic and R.P.U. Karunasiri, Phys. Rev. Lett. **66**, 3156 (1991).
- [16] Hong Yan, Phys. Rev. Lett. **68**, 3048 (1992).
- [17] J.H. Yao, C. Roland, and H. Guo, Phys. Rev. A **45**, 3903 (1992).
- [18] J. Krug and P. Meakin, Phys. Rev. E **47**, R17 (1993).
- [19] C. Tang and S. Liang, Phys. Rev. Lett. **71**, 2769 (1993).
- [20] J.H. Yao and H. Guo, Phys. Rev. E **47**, 1007 (1993).
- [21] P. Koblinski, A. Maritan, F. Toigo, and J.R. Banavar, Phys. Rev. Lett. **74**, 1783 (1995).
- [22] H. Huang, G.H. Gilmer, and T. Diaz de la Rubia, J. Appl. Phys. **84**, 3636 (1998).
- [23] J.T. Drotar, Y.-P. Zhao, T.-M. Lu, and G.-C. Wang, Phys. Rev. B **62**, 2118 (2000).
- [24] While the shadowing model used in Ref. [17] appears to correspond to a uniform flux distribution, the neglect of the cosine factor between the flux direction and the surface normal (see Ref. [13]) implies that the flux distribution is actually equivalent to the uniform angular distribution used in Ref. [19]. Similar considerations apply when comparing the grass model studied in Ref. [18] with continuum models.
- [25] G.H. Gilmer and E. Rubio (unpublished).
- [26] J.A. Stroschio, D.T. Pierce, M.D. Stiles, A. Zangwill, and L.M. Sander, Phys. Rev. Lett. **75**, 4246 (1995).
- [27] M. Matsushita and P. Meakin, Phys. Rev. A **37**, 3645 (1988).
- [28] P. Meakin, J. Phys. A **20**, L1113 (1987).
- [29] J. Krug and P. Meakin, Phys. Rev. A **40**, 2064 (1989).
- [30] Z. Racz and T. Vicsek, Phys. Rev. Lett. **51**, 2382 (1983).
- [31] For the two-bond triangular-lattice simulations shown, the values of the compactivity c , defined as the ratio of the number of deposited layers to the average film thickness were: $c=0.74$ (vertical deposition), $c=0.67$ (cosine distribution), and $c=0.63$ (uniform distribution).
- [32] B.B. Mandelbrot, *The Fractal Geometry of Nature* (Freeman, San Francisco, 1982).
- [33] F. Family and T. Vicsek, J. Phys. A **18**, L75 (1985).
- [34] The value $\alpha_2 \approx 1/2$ obtained for a cosine distribution is the same as obtained for ordinary ballistic deposition even though the Family-Vicsek scaling relation $\alpha = \beta/p$ does not hold.
- [35] J.G. Amar and F. Family, Phys. Rev. E **47**, 1595 (1993).
- [36] S. Das Sarma, S.V. Ghaisas, and J.M. Kim, Phys. Rev. E **49**, 122 (1994).
- [37] J.M. Lopez, Phys. Rev. Lett. **83**, 4594 (1999).
- [38] A. Barabasi, P. Szepefalusy, and T. Vicsek, Physica A **178**, 17 (1991).
- [39] T.A. Witten and L.M. Sander, Phys. Rev. Lett. **47**, 1400 (1981).